




# Preparation of highly conductive and flexible Ag-coated single fiberglass via dopamine functionalization and electroless depositing

Guoqiang Liu<sup>1,\*</sup> , Ningning Zhou<sup>2</sup>, and Qizhong Xiong<sup>3</sup>

<sup>1</sup>School of Materials Science and Engineering, Hefei University of Technology, Hefei 230009, Anhui, People's Republic of China

<sup>2</sup>Department of Chemical and Materials Engineering, Hefei University, Hefei 230601, People's Republic of China

<sup>3</sup>Anhui Province Key Laboratory of Farmland Ecological Conservation and Pollution Prevention, School of Resources and Environment, Anhui Agricultural University, Hefei 230036, Anhui, People's Republic of China

Received: 29 August 2020

Accepted: 13 December 2020

Published online:

2 January 2021

© The Author(s), under exclusive licence to Springer Science+Business Media, LLC part of Springer Nature 2021

## ABSTRACT

Flexible conductive glass fibers had widespread acquired attention in the field of electromagnetic interference shielding, sensor, and intelligent wearable devices. However, commercial fiberglass (FG) were insulators that greatly limit their application fields. Herein, flexible single FG with diameter of nearly 25  $\mu\text{m}$  was manufactured by a home-made equipment. Then the surface of FG was further functionalized by dopamine self-polymerization and formed a polydopamine linker layer to chelate Ag(I) ion. Finally, the consecutive silver nanoparticles were coated on PDM/FG (polydopamine/fiberglass) via electroless plating method (Ag-PDM/FG). The SEM, XPS, and XRD results demonstrated that the silver layer on the FG surface was compact, uniform, continuous, and in a metallic crystal state. The Ag-PDM/FG exhibited excellent electrical conductivity as high as  $2.49 \times 10^6 \text{ S m}^{-1}$  and could easily operate as a conductive wire for a LED device. Furthermore, the Ag-PDM/FG maintained its original conductivity even under various bending angles due to the stable Ag-coated layer. This work opens a new avenue for preparing flexible, continuous, and conductive FG with easy operation for wearable devices.

## 1 Introduction

The metallic layers (e.g., Ag, Cu, and Ni) supported on substrate of powders, fibers, fabrics, and microsphere materials had been attracted extensive attention owing to a series advantages of high

conductivity, wear resistance, chemical stability, and electromagnetic interference (EMI) shielding capacity [1–8]. Fiberglass (FG) reinforced composites exhibit excellent properties, including high strength, high modulus, and anti-corrosion, which had been widespread applied in many fields [9, 10]. In recently, several physicochemical modifications were devoted

Address correspondence to E-mail: gqliu@issp.ac.cn

to develop FG-based materials with novel characteristic for application in electric conductivity, color, luminescence, and sensor [11–14]. Many technologies had been implemented to prepare metallic coatings on substrate (e.g., FG, cotton), such as electrolytic deposition, sputtering, physical vapor deposition (PVD), and electroless plating [3]. However, the sputtering and PVD approaches were relied costly and complicated equipment, which severely limited their applications in large scale. Besides, compared with electroless plating route, the electrolytic plating technology suffered from series disadvantages of long-time expending, high price of power and less efficient during deposition process [2, 3, 15, 16]. In addition, the thickness and uniformity of metallic layer cannot be satisfied via using electrolytic plating method. It should be noted that the electroless plating technique was considered as a promising technique to generate metal-covered fabric owing to its advantages of operation-easy, cost-inexpensive, and environment-friendly [2, 17]. Until now, various mono-metals or alloys, including Ag, Cu, Ni, and Cu–Ni, had been plated on FG through electroless depositing strategy [17–22]. Liu investigated the effect of volume ( $\text{NH}_3\text{-H}_2\text{O}$ ) and deposition time on electroless plating of metallic nickel layer on glass-fabrics' surface. The volume resistivity of the glass fabric@nickel could reach as high as  $6.25 \times 10^{-3} \Omega \text{ cm}$  [21]. Xu et al. reported cobalt covering formed by electroless plating approach displayed excellent ferromagnetic performance with a saturation magnetization of 65 emu  $\text{g}^{-1}$  and improved coercivity up to 250 Oe, respectively [22].

Despite these achievements, conventional metal-coated FG composites usually limited by complicated activation and sensitization process, and costly noble metals (e.g.,  $\text{PdCl}_2$ ) [19–22]. Recently, surficial modified FG with functional group, such as  $-\text{NH}_2$ ,  $-\text{SH}$ , and  $-\text{COOH}$  [23–26], were alternatively developed to replace traditional activation-sensitization procedures. For instances, Liaw and coworkers explored the Ag layer supported on FG without roughening, sensitization, and activation processes. Instead, tetraethoxysilane was employed as modification reagent, which acted as a linker between silver ions and FG, result in a strong adhesion of Ag nanoparticles on FG [23]. Liu et al. reported a novel graphene-coated glass fiber composites with conductivity as high as  $4.5 \text{ S m}^{-1}$  and maintained original conductivity after different levels of bending through

electrostatic adsorption and hydroiodic acid reduction methods [24]. Kim et al. also presented a novel approach for the fabrication of conductive textiles coated with reduced graphene oxide. The conductive textiles exhibited a high electrical conductivity of  $1000 \text{ S m}^{-1}$  and maintained the conductivity under harsh conditions, such as repetitive twist for many times, low, and high temperatures [25].

Recently, great efforts had been devoted to prepare various conducting materials with merits of high electrical conductivity, low-cost and corrosion resistance for EMI and other potential applications [27, 28]. The conductive flexible fiber was a prospective candidate to form successive route for electric transmission with less dosage compared to that of powder materials. Meanwhile, the conductive fiber exhibited plenty merits in maintaining its original mechanical stability even under different bending extent, which could satisfy the demands of commercial application in field of flexible devices [25]. Furthermore, there several efforts were employed to modify and prepare conductive FG as conductor for promising fields [19–26], but a simple and effective method was still urgent for preparing functionalized FG. Specially, development of continuous and flexible FG as conductive wire for the emerging fields had become a new research topic.

In this study, FG with diameter of  $25 \mu\text{m}$  was prepared in our laboratory and immersed in dopamine aqueous solution (24 h, and pH of 8.5) to prepare an adhesive self-polymerized polydopamine coating on its surface. The polydopamine layer with abundant functional groups including  $-\text{OH}$ , and  $-\text{NH}_2$  served as a linker between FG and Ag(I) ions, which was favorable for the compact, continuous, and uniform Ag layer supported on FG via electroless plating method. The results prove that both the polydopamine layer and Ag particles were strong adhesion on surface of FG, and the electrical conductivity of Ag-PDM/FG could be as high as  $2.49 \times 10^6 \text{ S m}^{-1}$  and could keep still superior conductivity under different flexion angles. Moreover, Ag-PDM/FG was applied easily as a conductive wire for a LED device even after different levels of bending.

## 2 Experimental

### 2.1 Materials

The conventional alkali-free glass marble (E glass) was supplied by Zigong dengguan FG Co., Ltd (Sichuan, China). Silver nitrate (AR,  $\geq 99.0\%$ ,  $\text{AgNO}_3$ ), sodium hydroxide (AR,  $97.0\%$ ,  $\text{NaOH}$ ), seignette salt (AR,  $99.0\%$ ,  $\text{NaKC}_4\text{H}_4\text{O}_6$ ) and ammonium hydroxide (AR,  $25\text{--}28\%$ ,  $\text{NH}_4\text{OH}$ ) were purchased from Sinopharm Chemical Reagent Co., Ltd. 3-Hydroxytyramine hydrochloride ( $98.0\%$ , dopamine-HCl) was applied by Nanjing aoduofuni biotechnology Co., Ltd (Nanjing China). Tris (hydroxymethyl) ( $\geq 99.9\%$ ) was purchased from Sinopharm Chemical Reagent Co., Ltd. All the reagents in this experiment were used without any depuration.

### 2.2 Preparation of FG

Fiberglass (FG) was manufactured in a home-made equipment. First, alkali-free glass marble was put into a Pt–Rh alloy constructed crucible at temperature of  $1230\text{--}1260\text{ }^\circ\text{C}$ , and then the molten glass pulled from crucible to assemble on a winder with different rotation speed using water as sizing coated on it. The obtained FG was washed several times with acetone and deionized water, and then cut into  $2\text{--}4\text{ cm}$  for future use.

### 2.3 Polydopamine self-polymerization on FG

FG was immersed and stirred in dopamine aqueous solution for 24 h at room temperature in dark place with pH of 8.5 by adding tris. The concentration of dopamine in aqueous solution was 1.0, 1.5, 2.0, 2.5, 3.0, and  $4.0\text{ g L}^{-1}$ , respectively. The above polydopamine functionalized FG (PDM/FG) was washed several times with deionized water and dried under vacuum freeze-dried oven for 12 h.

### 2.4 Electroless plating of silver on surface of PDM/FG

Deposition silver thin layer on FG surface was operated by immersing PDM/FG in electroless plating bath of 100 mL containing seignette salt, ammonium hydroxide, and various concentration of silver nitrate ( $4.0, 8.0, 1.2, 1.6, 2.0\text{ g L}^{-1}$ ) at room temperature. First,

the ammonia was slowly dropped into silver nitrate aqueous solution until this mixed solution change into clarification again. Then, 1.0 g of PDM/FG were added into the above solution and stirred for 0.5 h. Finally, the seignette salt was added with the same concentration and volume of the silver nitrate. The obtained Ag-PDM/FG (Ag-polydopamine/FG) was washed by deionized water for several times and dried in  $\text{N}_2$  atmosphere thoroughly.

### 2.5 Characterization

The surface morphology of the as-prepared samples was investigated by a Phenom G2 Pro desktop Scanning Electron Microscope (SEM). The high magnification SEM images were observed by a S-4800 Microscope (Hitachi, Japan). The thickness of Ag layer was recorded through SU8010 Microscope (Hitachi, Japan). The FTIR spectra were investigated under transmission mode by a Nicolet 6700 spectrometer (Thermo Fisher, America). The roughness of PDM/FG was detected by Atomic Force Microscope (AFM, Nano Scope IV, USA). The XRD patterns were recorded by a D/max-2550 X-ray Diffractometer (Rigaku, Japan). The surface chemical structures were analyzed by an ESCALAB 250Xi X-ray Photoelectron Spectroscopy (Thermo, USA). Electrical conductivity of the obtained samples was investigated by a CHI660E electrochemical workstation.

### 2.6 Measurement electrical conductivity of Ag-PDM/FG

The electrical conductivity of Ag-PDM/FG was investigated by a CHI760E electrochemical workstation, and calculated through following equation [24].

$$K = L / R\pi(d/2)^2$$

$K$  conductivity,  $L$  length of Ag-PDM/FG,  $R$  the resistance of Ag-PDM/FG,  $d$  diameter of Ag-PDM/FG.

## 3 Results and discussion

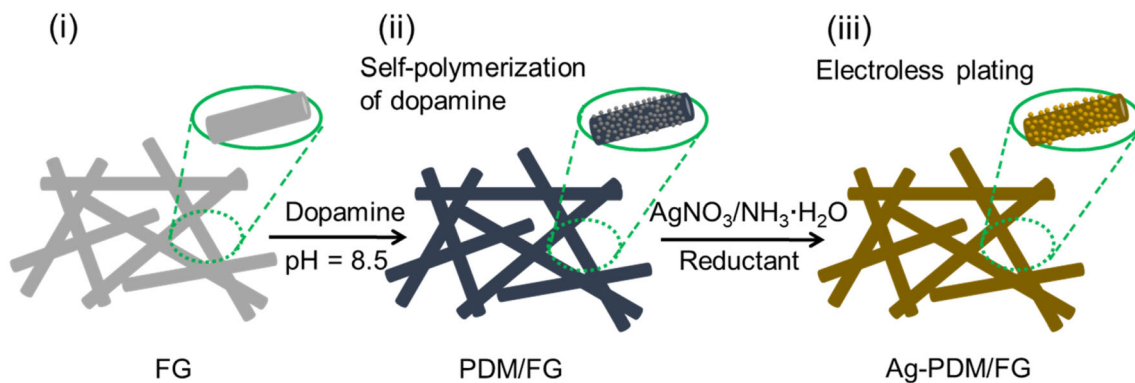
In this work, the fiberglass (FG) was manufactured by a home-made equipment. The digital image and schematic diagram were preliminarily exhibited in Fig. S1. Briefly, the FG was pulled from a Pt–Rh alloy constructed crucible with molten glass in it at

temperature around 1230–1260 °C, and then a winder was applied to assemble continuous FG. The diameter of FG could be simply controlled by the winder's rotation speed. As shown in Fig. S2, the SEM images of the obtained FG exhibits smooth surface with different assembling rate of winder, showing 7.5, 11.9, 17.1, and 25.0  $\mu\text{m}$  at rotation rate of 1000, 500, 300, and 200 rpm (revolution per minute), respectively.

The preparation procedure for Ag-PDM/FG was exhibited in Scheme 1. The conductive Ag-PDM/FG composite was prepared by next two consecutive processes: (i) FG was functionalized with dopamine molecules through a facile pH-induced dopamine self-polymerization strategy, resulting polydopamine coated on the surface of FG, and (ii) conductive Ag-PDM/FG was acquired using a room temperature chemical bath reduction (electroless plating) method using  $\text{AgNO}_3$  and seignette salt as metallic source and reducing agent, respectively. The SEM images of polydopamine-coated FG are exhibited in Fig. 1, as shown, with increasing the concentration of dopamine from 1.0 to 4.0  $\text{g L}^{-1}$ , the PDM/FG (polydopamine/fiberglass) exhibited obvious aggregation of small particles on FG surface (Fig. 1a–d). To date, the mechanism of dopamine in situ spontaneous oxidative polymerization was still not clear and a possible mechanism is shown in Fig. 1e [29]. Furthermore, the AFM images of PDM/FG at series self-polymerization time is exhibited in Fig. 2, compared to the smooth surface of clean FG (Fig. 2a), with the increase polymerization time, the roughness increases (Fig. 2b–d), which is favorable for grabbing more Ag(I) ion. PDM/FG was further investigated by energy dispersive X-ray spectroscopy (EDS). The SEM-EDS spectrum of the PDM/FG demonstrated that the surface was uniformly composed of C, O, Al,

Si, and Ca element, and the C element with relatively high atomic ratio could be attributed to polydopamine molecule (Fig. 2e–g). Moreover, the cross-sectional SEM images of PDM/FG were provided in Fig. S3 to investigate the thickness of polydopamine. From the SEM images, it could see clearly that the PDM was irregularly loaded or agglomerated on surface of FG, but the thickness of PDM was not obviously measured from the images due to the thin structure of PDM.

XPS was applied to investigate the chemical composition and valence structure of pure FG and PDM/FG. For pure FG, the survey XPS spectra revealed obvious signal of C 1s, Ca 2p, and O 1s (Fig. 3a). For PDM/FG, the survey XPS spectra exhibited the presence of C, N, and O element in sample (Fig. 3b). The enhanced single of C 1s and N 1s were attributed to dopamine self-polymerization on PDM/FG surface in comparison to pure FG. The above results confirmed that dopamine self-polymerization reaction had already happened and the polydopamine was successfully covered on the FG surface. In addition, the thickness of polydopamine coating above detecting depth of XPS technique result the single of Ca 2p disappear in survey XPS spectra. As shown in Fig. 3c, the curve fitted of high-resolution XPS spectra of N 1s from PDM/FG emerged two new peaks at binding energy of 398.7 eV and 400.0 eV, assigned to  $-\text{N}=\text{}$  and  $-\text{N}-\text{H}$  [30–32], respectively, while no obvious signal was received in pure FG sample. Based on above self-polymerization mechanism of dopamine (Fig. 1e), the  $=\text{N}-$  group was obtained from the reconstituted structure of dopamine derived the polydopamine molecule, while the  $-\text{N}-\text{H}$  bond was supplied by the amine group in the dopamine [33]. Figure 3d shows the spectra of C



**Scheme 1** Schematic illustration for preparing the Ag-PDM/FG

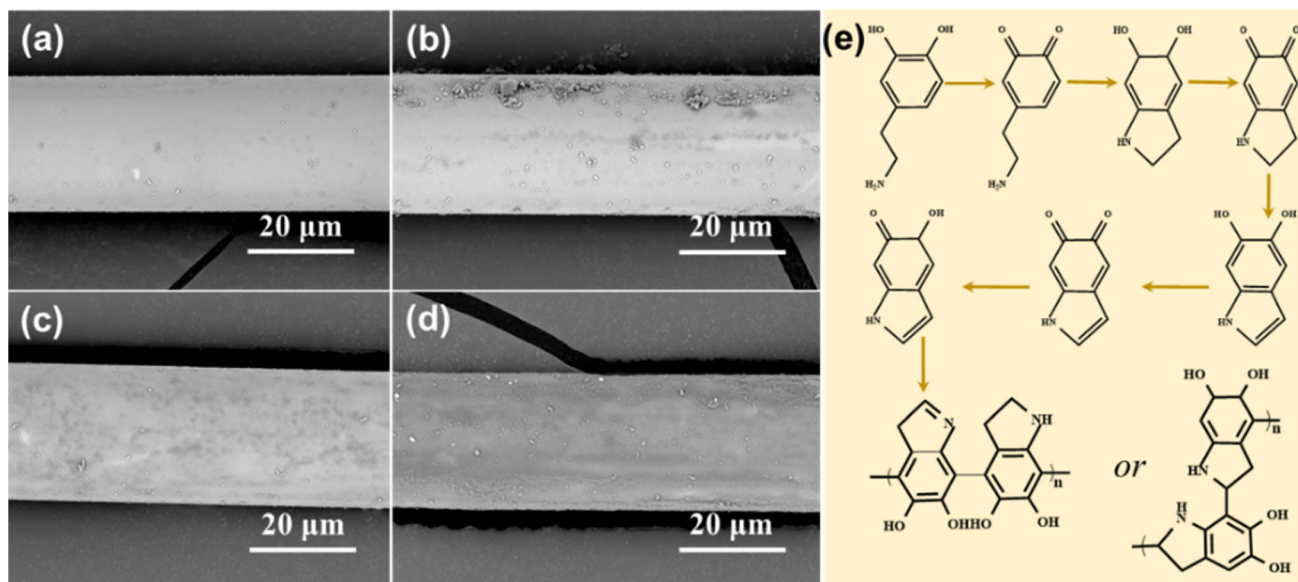


**Fig. 1** SEM images of the polydopamine-coated FG with different concentration of dopamine: **a**  $1.0 \text{ g L}^{-1}$ , **b**  $2.0 \text{ g L}^{-1}$ , **c**  $3.0 \text{ g L}^{-1}$ , and **d**  $4.0 \text{ g L}^{-1}$ . **e** Possible mechanism for dopamine's self-polymerization processes

1s from neat FG, two peaks at a binding energy of 284.8 eV and 286.4 eV, responding to C–C and C–O species [34]. For PDM/FG, there two new peaks were obtained compared to that of pure FG, with a binding energy at 285.4 eV and 288.3 eV, assigned to C–N and C=O species from polydopamine molecule [35, 36], respectively. The presence of abundant characteristic functional groups (e.g., C=O, C–N, –N–H, and =N–) of polydopamine from PDM/FG surface strongly indicated that the dopamine was successfully formed a thin film on FG. Further, the FTIR spectra of pure FG and PDM/FG were provided in Fig. S4. It could be clearly observed that the two obvious absorption peaks at wavenumbers of 928 and  $690 \text{ cm}^{-1}$  from pure FG appeared in Fig. S4, and new absorption peaks occurred at 1248, 1502 and  $1591 \text{ cm}^{-1}$ , attributing to the C–O stretching, phenylic C=C stretching, and N–H bending for series PDM/FG samples under different concentration of dopamine, respectively [37]. These results confirmed that the PDM was successfully modified on the surface of FG.

The SEM images of Ag-PDM/FG based on different concentrations of dopamine modified FG under a certain concentration of silver nitrate of  $12 \text{ g L}^{-1}$  are exhibited in Fig. 4. As shown, the polydopamine layer played an important role in the procedure for coating Ag nanoparticles on surface of FG. Deeper deposited polydopamine could results an increasing the silver particles loading due to increase the

number of species between the polydopamine and Ag(I) ions, which was favorable for the nucleation formation of silver nanoparticles. As a result, a compact, and uniform silver nanoparticle formed layer was supported on the surface of FG (Fig. S5). The XRD patterns of Ag-PDM/FG under different concentration of dopamine are exhibited in Figs. 5a and S6a and c. Explicitly, two strong diffraction peaks located at  $38.2^\circ$  and  $44.3^\circ$ , assigned to the (111) and (200) crystal planes of metallic silver [38–40]. For FG and PDM/FG, the broad diffraction peaks at around  $25^\circ$  was attributed to amorphous FG (Fig. 5a) [41]. In addition, the Ag-PDM/FG were obtained by ultrasound rinsing before electroless plating Ag layer which shown accordant results to those of free-ultrasound samples (for XRD results) (Fig. S6c). The high-resolution XPS spectra of Ag 3d in Ag-PDM/FG demonstrated that silver layer had been successfully supported on the FG surface with a strong peak of Ag (Figs. 5b and 6b, d). Specifically, the high-resolution XPS spectra of Ag 3d for series Ag-PDM/FG were displayed in Fig. S6b and d, two peaks at binding energy of 368.4 eV and 374.6 eV related to Ag 3d<sub>1/2</sub> and Ag 3d<sub>3/2</sub>, respectively, suggesting the presence of Ag (0) species [42]. The explicit peaks of XRD and XPS for series samples of Ag-PDM/FG confirm that the Ag layer forcefully adhered on surface of FG.

The electrical conductivity of Ag particle-coated FG was investigated by electrochemical workstation

**Fig. 2** AFM images of PDM/FG with different polymerization time: **a** 0 h, **b** 6 h, **c** 12 h, and **d** 24 h. **e** SEM-EDS spectrum of PDM/FG. **f** Analyzed area and **g** Atomic ratio of element

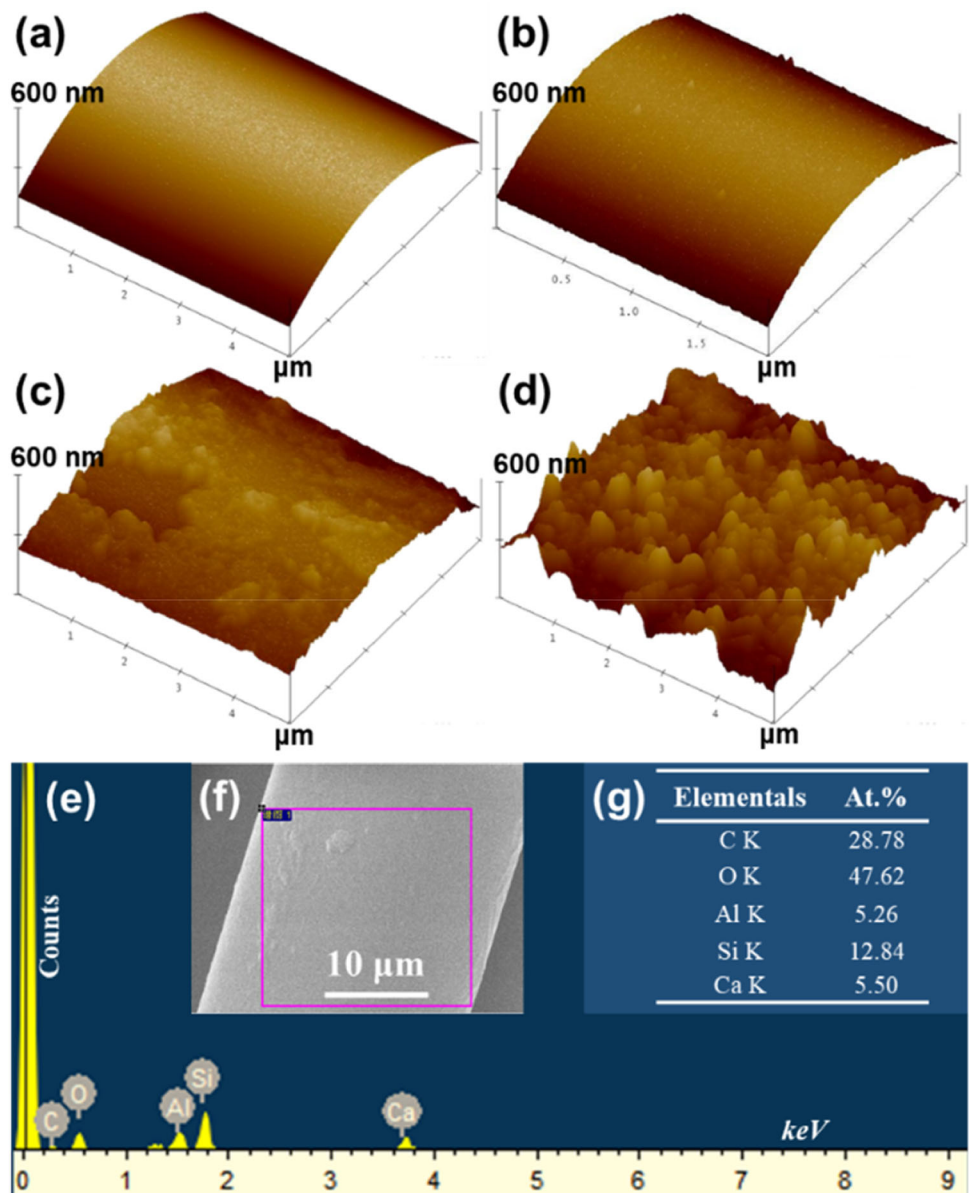


(Fig. S7). As shown in Fig. 6, an increasing electrical conductivity of Ag-PDM/FG could be obtained at the concentration region from 1.0 to 2.5 g L<sup>-1</sup> due to the enhanced loading of Ag layer, and reaching a value of  $2.30 \times 10^6$  S m<sup>-1</sup>. Nevertheless, further enhancement concentration of dopamine could not lead to further obvious increase of the electrical conductivity, suggesting that the thickness of Ag layer on the FG surface was not obviously changed. To investigate the binding force between PDM and FG, the PDM/FG was carried out electroless plating after ultrasound rinsing for 3 h (Fig. 6). The electrical conductivity of Ag-PDM/FG only show slight decrease compared to free-ultrasound one and reach as high as

$2.17 \times 10^6$  S m<sup>-1</sup>, indicating the strong compatibility of polydopamine on FG. The morphologies of Ag-PDM/FG synthesized by a 3.0 g L<sup>-1</sup> of dopamine modified FG and different concentrations of silver nitrate are shown in Fig. 7. With a low concentration of silver nitrate (e.g., 4.0 g L<sup>-1</sup>), the small and uncompact silver nanoparticles were distributed on the surface of PDM/FG (Fig. 7a). Further, an increasing concentration of silver nitrate in electroless plating bath from 8.0 to 20 g L<sup>-1</sup> (Fig. 7b–e), resulting an enhanced Ag nanoparticle, homogeneous and compact conductive layer on the PDM/FG surface (Fig. 7f). Moreover, the thickness of coated Ag layer was also investigated from cross-sectional SEM

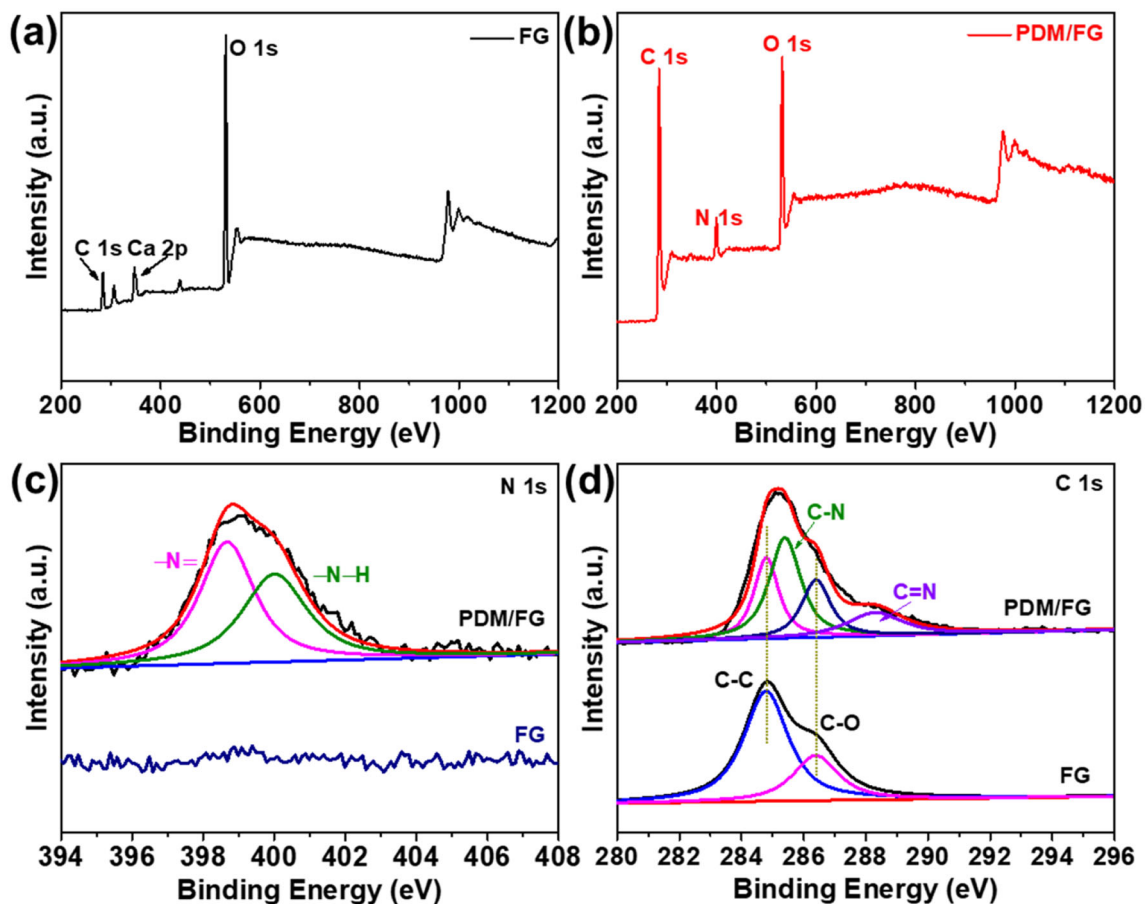


**Fig. 3** XPS survey of **a** FG and **b** PDM/FG. High-resolution XPS spectra of **c** N 1s and **d** C 1s in FG and PDM/FG

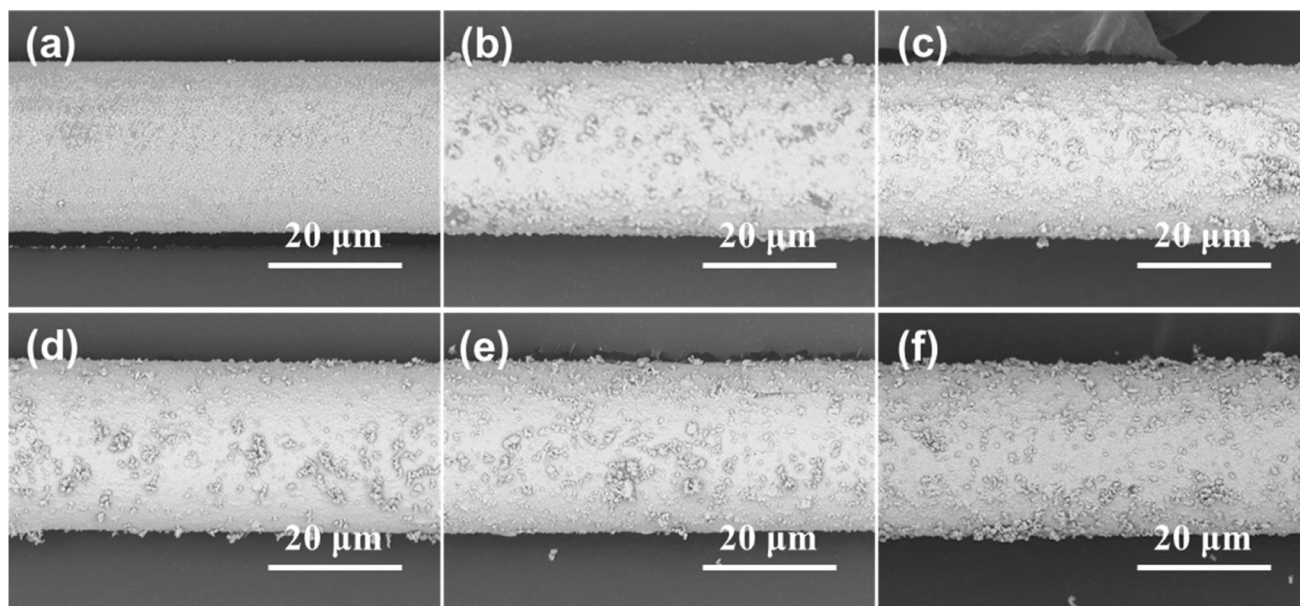


**Fig. 4** SEM images of Ag-PDM/FG at different concentration of dopamine: **a** 1.0 g L<sup>-1</sup>, **b** 1.5 g L<sup>-1</sup>, **c** 2.0 g L<sup>-1</sup>, **d** 2.5 g L<sup>-1</sup>, **e** 3.0 g L<sup>-1</sup>, **f** 4.0 g L<sup>-1</sup>, (concentration of silver nitrate was 12 g L<sup>-1</sup>)

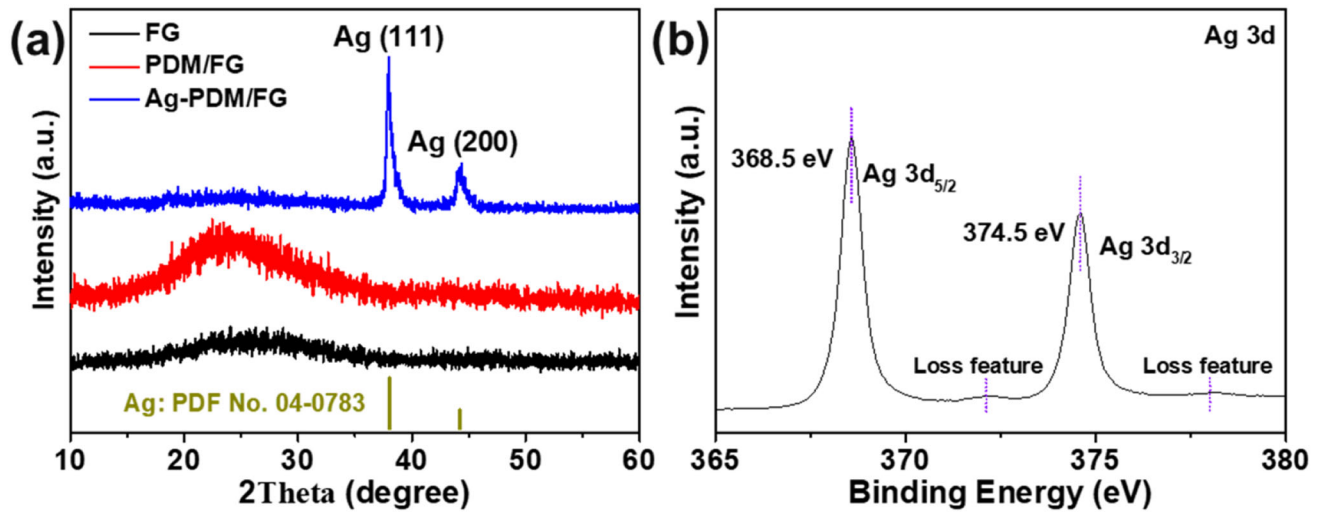
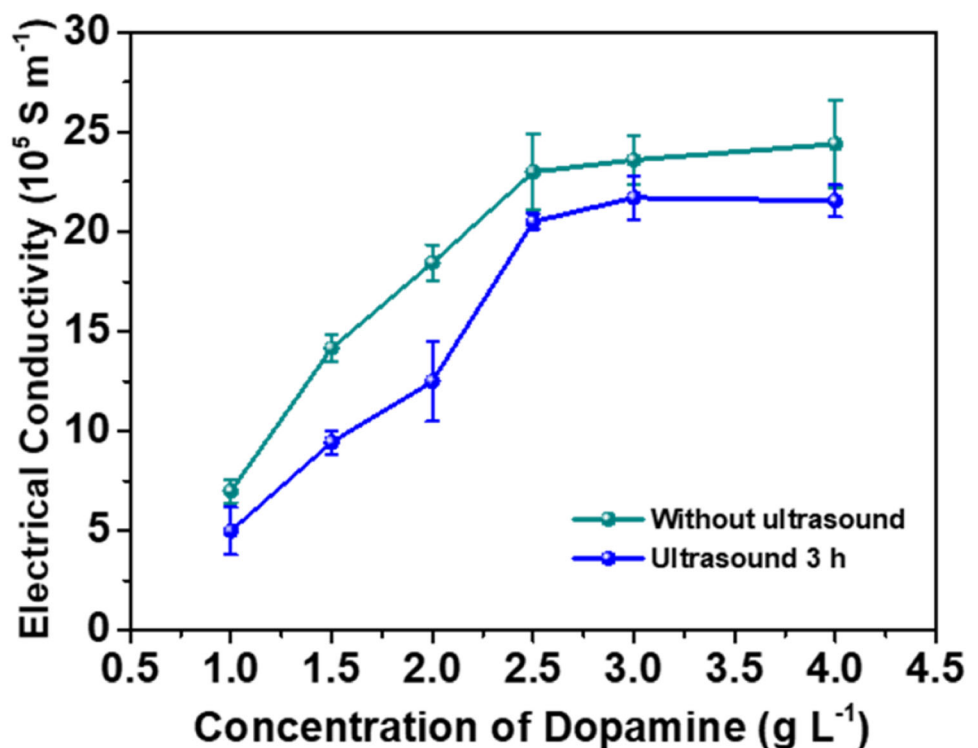


**Fig. 5** **a** XRD pattern of FG, PDM/FG, and Ag-PDM-FG. **b** High-resolution XPS spectra of Ag 3d in Ag-PDM/FG. ( $2.0 \text{ g L}^{-1}$  for concentration of dopamine,  $12.0 \text{ g L}^{-1}$  for concentration of silver nitrate)

**Fig. 6** Electrical conductivity of Ag-PDM/FG under different concentration of dopamine (concentration of silver nitrate =  $12 \text{ g L}^{-1}$ )



images (Fig. S8). The thicknesses of coated Ag film are 192, 236, 283, 297, and 310 nm for silver nitrate concentration of 4.0, 8.0, 12.0, 16.0, and  $20.0 \text{ g L}^{-1}$ , respectively ( $3.0 \text{ g L}^{-1}$  for concentration of dopamine). The thickness of Ag film increases rapidly at relatively low concentration of silver nitrate (less than

$12.0 \text{ g L}^{-1}$ ), while under high concentration of silver nitrate, the surface was already covered by sufficient Ag ion and result in the slowly increased thickness of Ag layer. Besides, the XRD and XPS data of Ag-PDM/FG samples under different concentration of silver nitrate are also investigated (Fig. S9) and



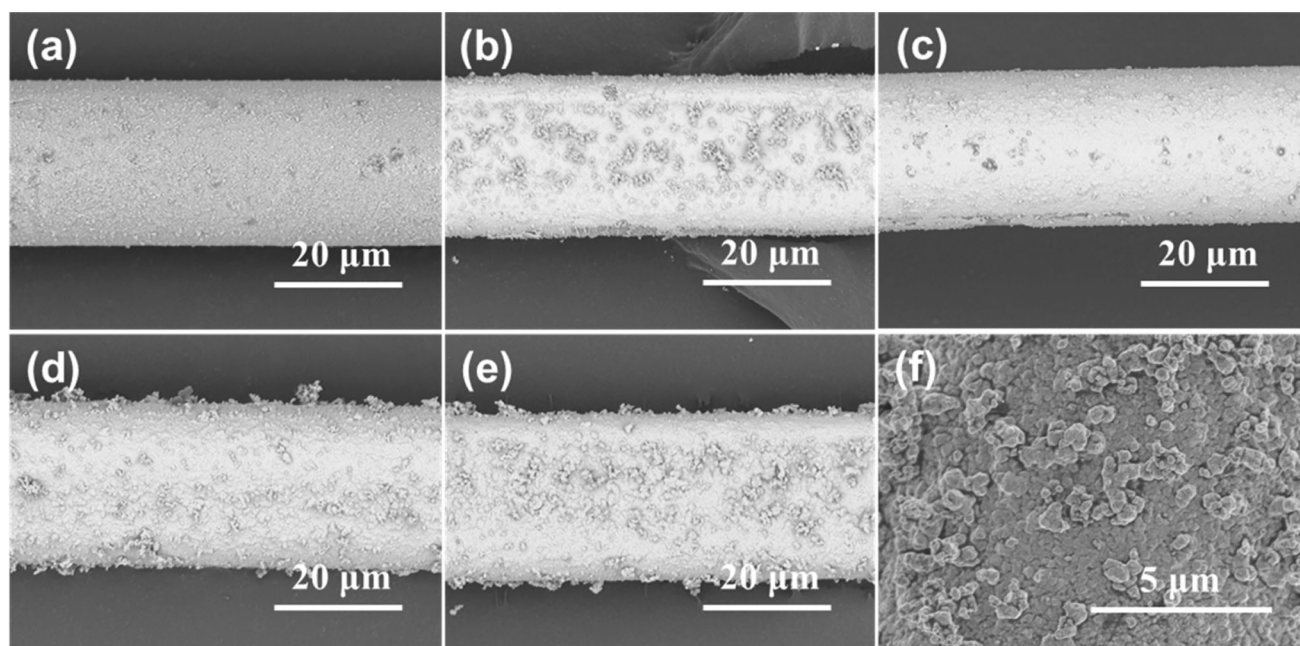


**Fig. 7** SEM images of Ag-PDM/FG at different concentration of silver nitrate: **a** 4.0 g L<sup>-1</sup>, **b** 8.0 g L<sup>-1</sup>, **c** 12.0 g L<sup>-1</sup>, **d** 16 g L<sup>-1</sup>, **e** 20.0 g L<sup>-1</sup>. **f** Enlarged SEM image from **e** (concentration of dopamine is 3.0 g L<sup>-1</sup>)

exhibited consistent results to those of other Ag-PDM/FGs. In addition, the SEM images of before and after ultrasound for 2 h without obvious structure degradation proved that the Ag layer was strongly adhered on FG surface (Fig. S10).

The electrical conductivity of Ag-PDM/FG under various concentration of silver nitrate are exhibited in Fig. 8a. As shown, the electrical conductivity of Ag-PDM/FG rapid increase with the high concentration of silver nitrate. However, the electrical conductivity shown slightly improvement (from  $2.32 \times 10^6 \text{ S m}^{-1}$ ) when silver concentration more than 12.0 g L<sup>-1</sup> due to the saturated Ag coating and delivered optimal conductivity of  $2.49 \times 10^6 \text{ S m}^{-1}$ . At low level concentration of silver nitrate, Ag ions grabbed by functional groups in PDM was insufficient, when silver nitrate concentration achieved high level, the Ag ions may grab in groups sufficiently. In a word, with assistant of polydopamine, the Ag particles were successfully plated on FG surface. Further, the Ag-PDM/FG maintained original conductive capacity after different levels of bending due to its excellent flexibility, as well as suggesting the stable Ag layer on FG (Fig. 8b). The obtained Ag-PDM/FG could easily operate as a conductive wire for a LED light even under various bending angles, indicating its

promising application in intelligent electronic devices (Fig. 8c).

#### 4 Conclusions

FG with diameter of around 25 μm was successfully manufactured in our laboratory. A uniform and rough polydopamine layer was adhered on surface of FG by a facile and effective self-polymerization approach. PDM assisted electroless plating strategy was developed to form compact and conductive Ag nanoparticles layer strong adhesion on FG even under ultrasound for 3 h. The morphologies of metallic FG could be influenced by concentration of dopamine and silver nitrate, resulting a maximum electrical conductivity of  $2.49 \times 10^6 \text{ S m}^{-1}$ . The Ag-PDM/FG could keep original electrical conductivity even under different bending angles and easily operate as a conductive wire for LED device. Our works may open a new avenue for preparing flexible, and continuous, and conductive FG with easily operated as conductive wire for wearable devices.

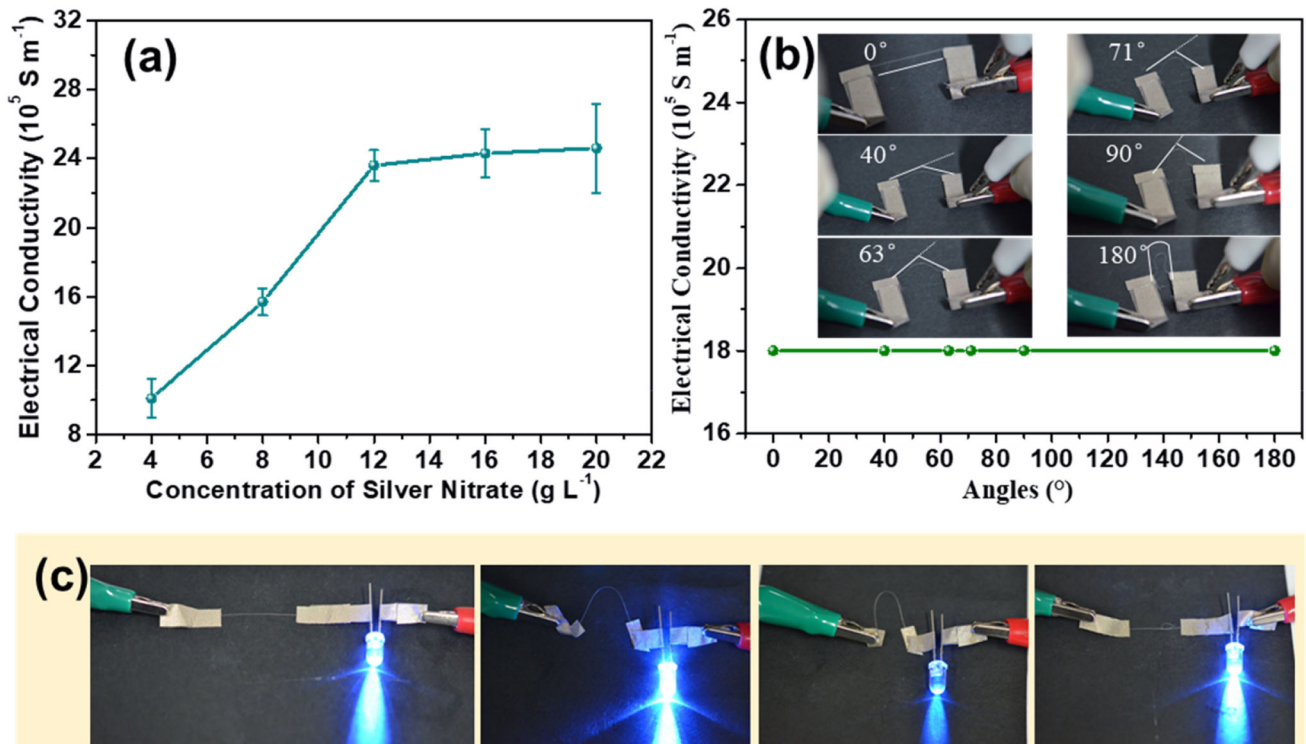


**Fig. 8** **a** Electrical conductivity of Ag-PDM/FG at different concentration of silver nitrate. **b** Electrical conductivity of Ag-PDM/FG under various bending angles (concentration of

dopamine and silver nitrate were  $2.0 \text{ g L}^{-1}$  and  $12 \text{ g L}^{-1}$ , respectively). **c** The digital photos of lightened LED by Ag-PDM/FG as conductive wire under different bending angles

## Acknowledgements

The authors acknowledge the Fundamental Research Funds for the Central Universities, the Talent Scientific Research Foundation of Hefei University (Grant No. 18-19RC22), the Natural Science Foundation of Anhui Province (Grant No. 1908085QC139), the Youth Science Fund of Anhui Agricultural University (Grant No. 2018zd25).

## Compliance with ethical standards

**Conflict of interest** The authors declare that they have no conflict of interest.

**Supplementary Information:** The online version of this article (<https://doi.org/10.1007/s10854-020-05112-w>) contains supplementary material, which is available to authorized users.

## References

1. J. Cai, C. Zhang, A. Khan, L. Wang, W.D. Li, Selective electroless metallization of micro- and nanopatterns via

- poly(dopamine) modification and palladium nanoparticle catalysis for flexible and stretchable electronic applications. *ACS Appl. Mater. Interfaces* **10**, 28754–28763 (2018)
2. X. Ding, Y. Wang, R. Xu, Q. Qi, W. Wang, D. Yu, Layered cotton/rGO/NiWP fabric prepared by electroless plating for excellent electromagnetic shielding performance. *Cellulose* **26**, 8209–8223 (2019)
3. O. Güler, T. Varol, Ü. Alver, The effect of flake-like morphology on the coating properties of silver coated copper particles fabricated by electroless plating. *J. Alloy. Compd.* **782**, 679–688 (2019)
4. M. Gao, W. Lu, B. Yang, S. Zhang, J. Wang, High corrosion and wear resistance of Al-based amorphous metallic coating synthesized by HVAF spraying. *J. Alloy. Compd.* **735**, 1363–1373 (2018)
5. H.K. Choudhary, R. Kumar, S.P. Pawar, U. Sundararaj, B. Sahoo, Effect of morphology and role of conductivity of embedded metallic nanoparticles on electromagnetic interference shielding of PVDF carbonaceous-nanofiller composites. *Carbon* **164**, 357–368 (2020)
6. S.P. Pawar, S. Stephen, S. Bose, V. Mittal, Tailored electrical conductivity, electromagnetic shielding and thermal transport in polymeric blends with graphene sheets decorated with

- nickel nanoparticles. *Phys. Chem. Chem. Phys.* **17**, 14922–14930 (2015)
7. R. Kumar, H.K. Choudhary, A.V. Anupama, A.V. Menon, S.P. Pawar, S. Bose, B. Sahoo, Nitrogen doping as a fundamental way to enhance the EMI shielding behavior of cobalt particle-embedded carbonaceous nanostructures. *New J. Chem.* **43**, 5568–5580 (2019)
  8. R. Kumar, H.K. Choudhary, S.P. Pawar, S. Bose, B. Sahoo, Carbon encapsulated nanoscale iron/iron-carbide/graphite particles for EMI shielding and microwave absorption. *Phys. Chem. Chem. Phys.* **19**, 23268–23279 (2017)
  9. D. Ren, K. Li, L. Chen, S. Chen, M. Han, M. Xu, X. Liu, Modification on glass fiber surface and their improved properties of fiber-reinforced composites *via* enhanced interfacial properties. *Compos. Part B* **177**, 107419–107429 (2019)
  10. B.A. Patterson, C.E. Busch, M. Bratcher, J. Cline, D.E. Harris, K.A. Masser, A.L. Fleetwood, Influence of temperature dependent matrix properties on the high-rate impact performance of thin glass fiber reinforced composites. *Compos. Part B* **192**, 108009–108018 (2020)
  11. X. Huang, Z. Fang, Z. Peng, Z. Ma, H. Guo, J. Qiu, G. Dong, Formation, element-migration and broadband luminescence in quantum dot-doped glass fibers. *Opt. Express* **25**, 19691–19670 (2017)
  12. L. Groo, J. Nasser, L. Zhang, K. Steinke, D. Inman, H. Sodano, Laser induced graphene in fiberglass-reinforced composites for strain and damage sensing. *Compos. Sci. Technol.* **199**, 108367–110876 (2020)
  13. Z. Liu, Q. Zhang, H. Wang, Y. Li, Magnetic field induced formation of visually structural colored fiber in micro-space. *J. Colloid Interf. Sci.* **406**, 18–23 (2013)
  14. X. Liu, Y. Wang, Z. Chen, K. Ben, Z. Guan, A self-modification approach toward transparent superhydrophobic glass for rainproofing and superhydrophobic fiberglass mesh for oil–water separation. *Appl. Surf. Sci.* **360**, 789–797 (2016)
  15. H. Chen, Y. Tai, C. Xu, Fabrication of copper-coated glass fabric composites through electroless plating process. *J. Mater. Sci.* **28**, 798–802 (2017)
  16. J. Zhang, J. Li, G. Tan, R. Hu, J. Wang, C. Chang, X. Wang, Thin and flexible Fe-Si-B/Ni-Cu-P metallic glass multilayer composites for efficient electromagnetic interference shielding. *ACS Appl. Mater. Interfaces* **9**, 42192–42199 (2017)
  17. C. Xu, R. Zhou, H. Chen, X. Hou, G. Liu, Y. Liu, Silver-coated glass fibers prepared by a simple electroless plating technique. *J. Mater. Sci.* **25**, 4638–4642 (2014)
  18. C. Xu, G. Liu, H. Chen, R. Zhou, Y. Liu, Fabrication of conductive copper-coated glass fibers through electroless plating process. *J. Mater. Sci.* **25**, 2611–2617 (2014)
  19. Y.-W. Nam, J.-H. Choi, W.-J. Lee, C.-G. Kim, Fabrication of a thin and lightweight microwave absorber containing Ni-coated glass fibers by electroless plating. *Compos. Sci. Technol.* **145**, 165–172 (2017)
  20. J. Lee, B.M. Jung, S.B. Lee, S.K. Lee, K.H. Kim, FeCoNi coated glass fibers in composite sheets for electromagnetic absorption and shielding behaviors. *Appl. Surf. Sci.* **415**, 99–103 (2017)
  21. Y. Tai, H. Chen, C. Xu, Y. Liu, Conductive glass fabrics@nickel composites prepared by a facile electroless deposition method. *Mater. Lett.* **171**, 158–161 (2016)
  22. Y. Tai, H. Chen, C. Xu, Y. Liu, Glass fabric@cobalt core-shell composites: electroless plating fabrication and their enhanced magnetic properties. *Mater. Lett.* **188**, 80–83 (2017)
  23. W.-F. Lien, P.-C. Huang, S.-C. Tseng, C.-H. Cheng, S.-M. Lai, W.-C. Liaw, Electroless silver plating on tetraethoxy silane-bridged fiber glass. *Appl. Surf. Sci.* **258**, 2246–2254 (2012)
  24. G. Liu, F. Shi, Y. Li, Q. Zhang, H. Wang, Preparation and electrical properties of graphene coated glass fiber composites. *J. Inorg. Mater.* **30**, 763–768 (2015)
  25. Y.J. Yun, W.G. Hong, W.-J. Kim, Y. Jun, B.H. Kim, A novel method for applying reduced graphene oxide directly to electronic textiles from yarns to fabrics. *Adv. Mater.* **25**, 5701–5705 (2013)
  26. S.-D. Kim, W. Choe, J. Choi, J.-R. Jeong, Preparation and characterization of silver coated magnetic microspheres prepared by a modified electroless plating process. *Powder Technol.* **342**, 301–307 (2019)
  27. H.K. Choudhary, R. Kumar, S.P. Pawar, A.V. Anupama, S. Bose, B. Sahoo, Effect of coral-shaped yttrium iron garnet particles on the EMI shielding behaviour of yttrium iron garnet-polyaniline-wax composites. *ChemistrySelect* **3**, 2120–2130 (2018)
  28. H.K. Choudhary, R. Kumar, S.P. Pawar, U. Sundararaj, B. Sahoo, Enhancing absorption dominated microwave shielding in Co@C–PVDF nanocomposites through improved magnetization and graphitization of the Co@C-nanoparticles. *Phys. Chem. Chem. Phys.* **21**, 15595–15608 (2019)
  29. W. Wang, R. Li, M. Tian, L. Liu, H. Zou, X. Zhao, L. Zhang, Surface silverized meta-aramid fibers prepared by bio-inspired poly(dopamine) functionalization, *ACS Appl. Mater. Interfaces* **5**, 2062–2069 (2013)
  30. W. Cai, J. Wang, Y. Pan, W. Guo, X. Mu, X. Feng, B. Yuan, X. Wang, Y. Hu, Mussel-inspired functionalization of electrochemically exfoliated graphene: based on self-polymerization of dopamine and its suppression effect on the fire hazards and smoke toxicity of thermoplastic polyurethane. *J. Hazard. Mater.* **352**, 57–69 (2018)
  31. N.G.P. Chew, S. Zhao, C. Malde, R. Wang, Polyvinylidene fluoride membrane modification *via* oxidant-induced

- dopamine polymerization for sustainable direct-contact membrane distillation. *J. Membr. Sci.* **563**, 31–42 (2018)
32. W. Wang, W. Cheng, M. Tian, H. Zou, L. Li, L. Zhang, Preparation of PET/Ag hybrid fibers via a biomimetic surface functionalization method. *Electrochim. Acta* **79**, 37–45 (2012)
  33. F. Yu, S. Chen, Y. Chen, H. Li, L. Yang, Y. Chen, Y. Yin, Experimental and theoretical analysis of polymerization reaction process on the polydopamine membranes and its corrosion protection properties for 304 stainless steel. *J. Mol. Struct.* **982**, 152–161 (2010)
  34. C. Xu, M. Tian, L. Liu, H. Zou, L. Zhang, W. Wang, Fabrication and properties of silverized glass fiber by dopamine functionalization and electroless plating. *J. Electrochem. Soc.* **159**(4), D217–D224 (2012)
  35. Y. Fu, L. Liu, L. Zhang, W. Wang, Highly conductive one-dimensional nanofibers: silvered electrospun silica nanofibers *via* poly(dopamine) functionalization. *ACS Appl. Mater. Interfaces* **6**, 5105–5112 (2014)
  36. Q. Li, M. Tian, L. Liu, H. Zou, L. Zhang, W.C. Wang, Facile preparation of Fe<sub>2</sub>O<sub>3</sub>@Ag core-shell structured nanoparticles. *Electrochim. Acta* **91**, 114–121 (2013)
  37. L. Yu, J. Zhao, L. Shen, Y. Gao, X. Wang, Ag-coated PAN nanofibers prepared by poly(dopamine)-assisted electroless plating. *Adv. Mat. Res.* **482–484**, 2543–2546 (2012)
  38. X. Zhang, H. Sun, S. Tan, J. Gao, Y. Fu, Z. Liu, Hydrothermal synthesis of Ag nanoparticles on the nanocellulose and their antibacterial study. *Inorg. Chem. Commun.* **100**, 44–50 (2019)
  39. D. Kumar, S. Singh, N. Khare, Plasmonic Ag nanoparticles decorated NaNbO<sub>3</sub> nanorods for efficient photoelectrochemical water splitting. *Int. J. Hydrogen Energy* **43**, 8198–8205 (2018)
  40. H. Huang, L. Xia, X. Shi, A.M. Asiri, X. Sun, Ag nanosheets for efficient electrocatalytic N<sub>2</sub> fixation to NH<sub>3</sub> under ambient condition. *Chem. Commun.* **54**, 11427–11430 (2018)
  41. A.J. Jafari, R.R. Kalantary, A. Esrafil, H. Arfaeinia, Synthesis of silica-functionalized graphene oxide/ZnO coated on fiberglass and its application in photocatalytic removal of gaseous benzene. *Process Saf. Environ.* **116**, 377–387 (2018)
  42. C.-Y. Lee, Y. Zhao, C. Wang, D.R.G. Mitchell, G.G. Wallace, Rapid formation of self-organised Ag nanosheets with high efficiency and selectivity in CO<sub>2</sub> electroreduction to CO. *Sustain. Energy Fuels* **1**, 1023–1027 (2017)

**Publisher's Note** Springer Nature remains neutral with regard to jurisdictional claims in published maps and institutional affiliations.